X-735-68-400

NASA TM X- 63425

NICKEL POWDERS AND PLAQUES FOR NICKEL-CADMIUM CELL PLATES

GERALD HALPERT

OCTOBER 1968

GSFC — GODDARD SPACE FLIGHT CENTER
GREENBELT, MARYLAND

X-735-68-400

NICKEL POWDERS AND PLAQUES

FOR

NICKEL-CADMIUM CELL PLATES

Gerald Halpert
Systems Division

October 1968

GODDARD SPACE FLIGHT CENTER
Greenbelt, Maryland

NICKEL POWDERS AND PLAQUES

FOR

NICKEL-CADMIUM CELL PLATES

Gerald Halpert
Systems Division

ABSTRACT

Nickel powders and plaques are being investigated in an effort to develop more uniform and predictable battery-plate materials for nickel-cadmium aerospace cells. Two aspects of this effort are described herein: the development of uniform materials, and the characterization and effect of changes in the materials during operation. Average particle sizes of the nickel powders used in the manufacturing of plaques are determined by using the Fisher sub-sieve sizing method and by use of the scanning electron microscope. Photographs of the nickel powders and plaques are described.

CONTENTS

ILLUSTRATIONS

TABLE

NICKEL POWDERS AND PLAQUES

FOR

NICKEL-CADMIUM CELL PLATES

INTRODUCTION

A program to develop uniform and predictable battery materials for nickel-cadmium aerospace cells was undertaken in July of this year. The effort has been divided into two segments: the development of uniform materials, being carried out under contract to Tyco Laboratories, Waltham, Mass. (NAS-5-11561) under Project Scientist Dr. J. Parry; and the characterization and effect of changes in the materials during operation, being conducted in the GSFC Materials Research and Development Branch.

During the first quarter of the program, a survey of the secondary battery materials was made and a bibliography was compiled.* The first-quarterly report (September 1968) of the Tyco contract contains a survey of the manufacturing processes and a materials evaluation based on the literature and interviews with representatives of battery manufacturers.

As a first step in the materials evaluation and characterization, it was important to determine the variations in the nickel powders as received from the only source of suitable carbonyl nickel - the International Nickel Company. To establish this, samples of these nickel powders, as used by various battery manufacturers in the production of the sintered plaques that eventually become nickel and cadmium plates, were submitted to Tyco and GSFC for characterization.

This report gives the results of the GSFC characterization of average particle size using the Fisher ASTM method. Also included are enlarged photos of the nickel powders from both Inco and the Sherritt Gordon Company of Canada; photos from the scanning electron microscope show both sides of a typical sintered nickel plaque.

FISHER AVERAGE-PARTICLE-SIZE ANALYSIS

The Fisher Sub Sieve Sizer measurement technique is based on the principle that air flows more readily through a bed of coarse powder than through fine powder having equal bed shape,

*G. H. Halpert and W. H. Webster, Jr., "Bibliography of Secondary Aerospace Batteries and Battery Materials," forthcoming NASA Special Publication. (NASA-SP's are available from the Clearinghouse for Federal Scientific and Technical Information, Springfield, Virginia 22151).

Table 1

Fisher Average Particle Diameter

Sample Number	Fisher Porosity (Ratio of Air Space to Volume)	Average Particle Size (Microns)
704-1* #287	.756	3.22
2* #255	.757	2.82
3	.791	2.63
4	.752	3.27
5	.747	3.21
6	.750	3.23
7	.757	3.39
8	.751	3.18
9	.759	2.93
10	.758	3.18
11	.757	3.18
12	.752	3.16
13	.760	3.23
14* #255	.778	2.78
15* #287	.771	3.14
16† #826	.792	2.17
17† #692	.798	3.58
18	.737	3.50

*Inco specimens.
†Sherritt specimens.

apparent volume, and percent of voids. The difference in air flow is due to average pore diameter and total interstitial surface, both of which are functions of the average particle size.* The method does not provide an exact measurement, but rather, a relative comparison of powder particle sizes.

The results of the Fisher particle-size analysis are given in Table 1. A sample of powder equal to the density of nickel (8.90 g/cc) was packed into a column under a pressure of 100 psi. The porosity, the ratio of air space in the sample bed to total volume occupied by the packed sample, is read directly from a chart attached to the instrument. This is also the case for the average particle size in microns. The values given are the average of two to four samples. The deviation in porosity is ±0.01 and the deviation in particle diameter is ±0.05. The specific surface in square meters per gram is equal to 6.0 divided by the average particle diameter in microns.

The samples were supplied by Inco, Sherritt Gordon, and the nickel-cadmium battery manufacturers. Samples 704-1 and 704-15 are Inco #287 powders; samples 704-2 and 704-14 are Inco #255 powders. These powders have been used extensively in the production of nickel plaques for nickel and cadmium plates. Sherritt Gordon powders are 704-16 (#826) and 704-17 (#692). The other samples will remain unidentified unless specifically requested by a battery manufacturer concerned about their sample.

ELECTRON SCANNING OF POWDERS

Inco powders #287 and #255, Sherritt Gordon powders #692 and #826, and two sides of a typical sintered nickel plaque were subjected to microscopic characterization. For better resolution and depth of field, a Stereoscan Electron Microscope, Series 1 (Cambridge Instrument Company of England) was used. The photos are given in Figures 1 through 16.

*The technique is described in ASTM Specification B330-65.

Inco #255 powders are given in Figures 1 to 3 at magnifications of 2300X, 5700X and 7600X. These can be compared with Inco #287 powders at comparable magnifications given in Figures 4 to 6. It can be seen that while both types of powder contain long spiney particles with sharp points the #287 particles appear to be thicker than the #255 powders. This agrees with the higher Fisher particle-size measurements for the #287 powders.

Samples of Sherritt Gordon powders #692 and #826 appear in Figures 7 and 8. These differ from the Inco powders in that they are more spherical. In these photos the #692 particles appear larger than the #826 particles; this is also consistent with the Fisher particle-size data.

A typical nickel plaque is shown in Figures 9 through 16. The smooth side of the plaque is shown in Figures 9 through 12. It is interesting to note the distribution in pore size and characteristics of surface structure in Figures 9 and 10. The largest pore given in Figure 9 is 60 microns in diameter. It is also interesting to note in Figures 11 and 12 that in the process of sintering, the surface structure of the particles has become smoother. These effects are also noted in the opposite side of the plaque which appears to the naked eye to be considerably rougher than the first side and yet appears more similar to it when magnified.

CONCLUSIONS

1. The average particle diameters for the Inco #255 and #287 powders are sufficiently different to be readily distinguishable.

2. Determination of the average particle diameter using the Fisher Sub Sieve Sizer, although not an absolute technique, is accurate enough for use as a measurement technique in the selection and control of battery powders used in the fabrication of porous nickel plaques.

3. The scanning electron microscope is a useful tool in observing surface characteristics and particle shape of nickel powders.

4. It is also useful in observing the fabricated nickel plaque structure in order to determine the effects of different fabricating techniques and variation in pore structure.

ACKNOWLEDGMENT

The author wishes to thank William Campbell for his assistance with the Fisher analysis and Robert Anstead for his assistance with the scanning electron microscope.

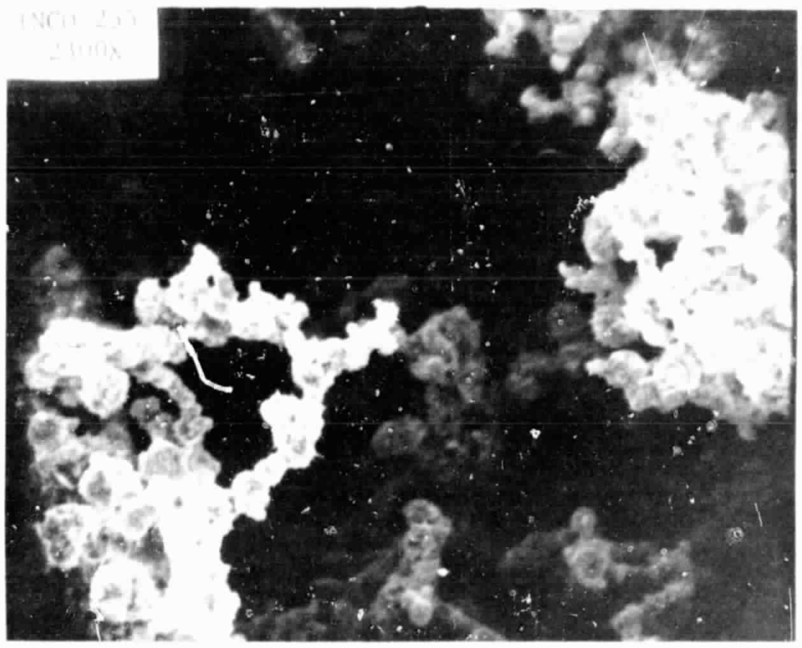

Figure 1—Inco No. 255 at 2300X.

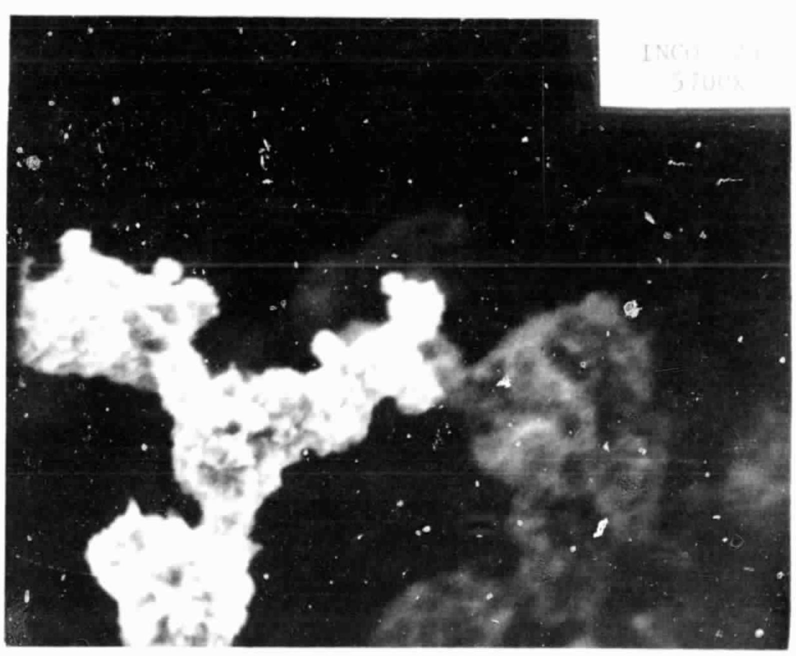

Figure 2—Inco No. 255 at 5700X.

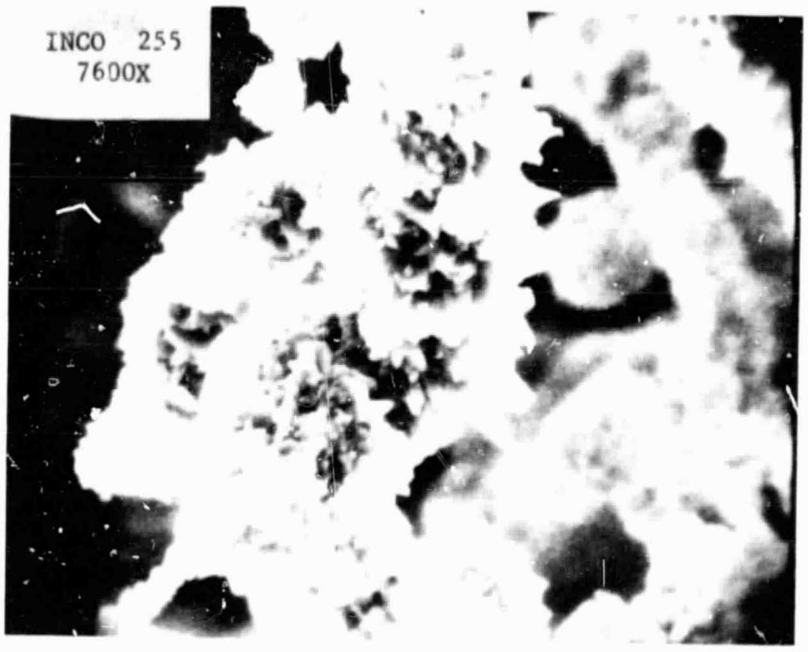

Figure 3—Inco No. 255 at 7600X.

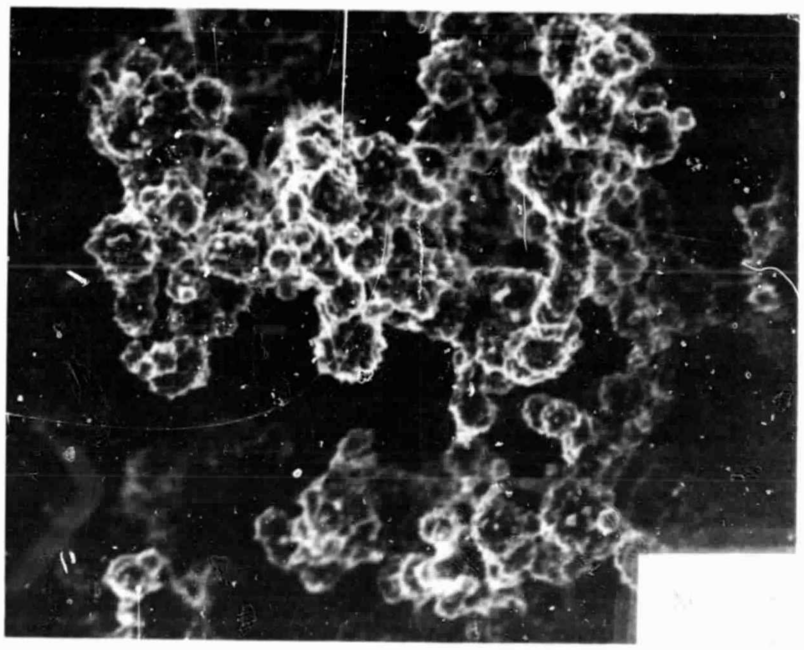

Figure 4—Inco No. 287 at 2300X.

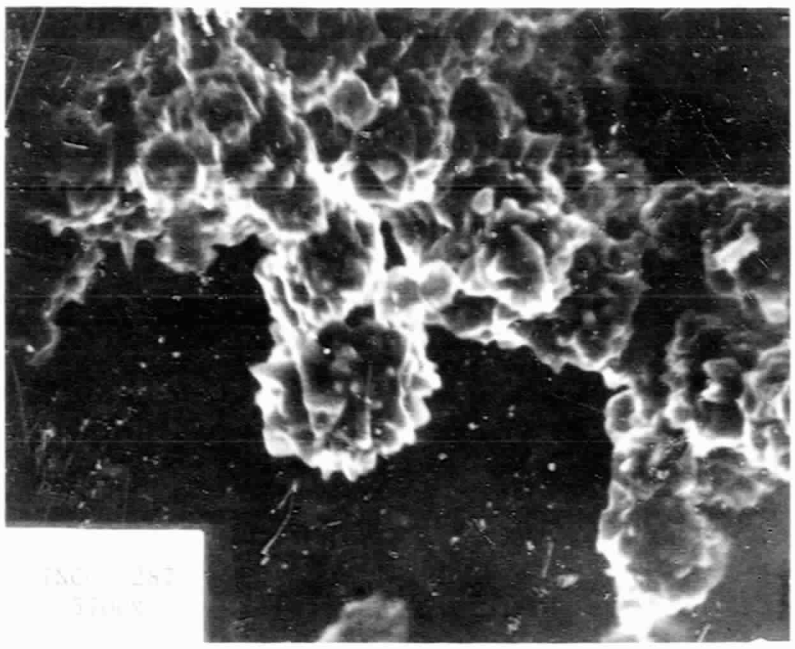

Figure 5—Inco No. 287 at 5700X.

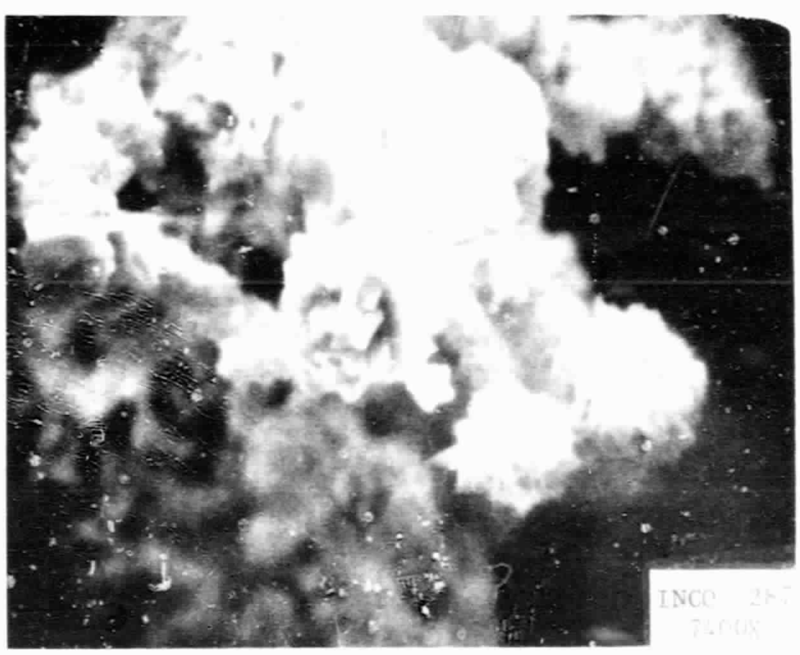

Figure 6—Inco No. 287 at 7400X.

Figure 7—Sherritt No. 692 at 3000X.

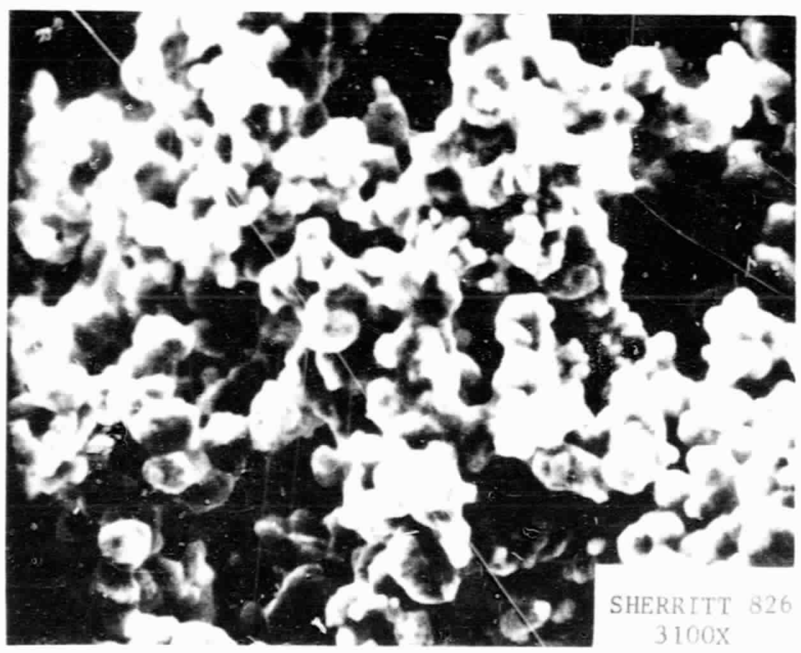

Figure 8—Sherritt No. 826 at 3100X.

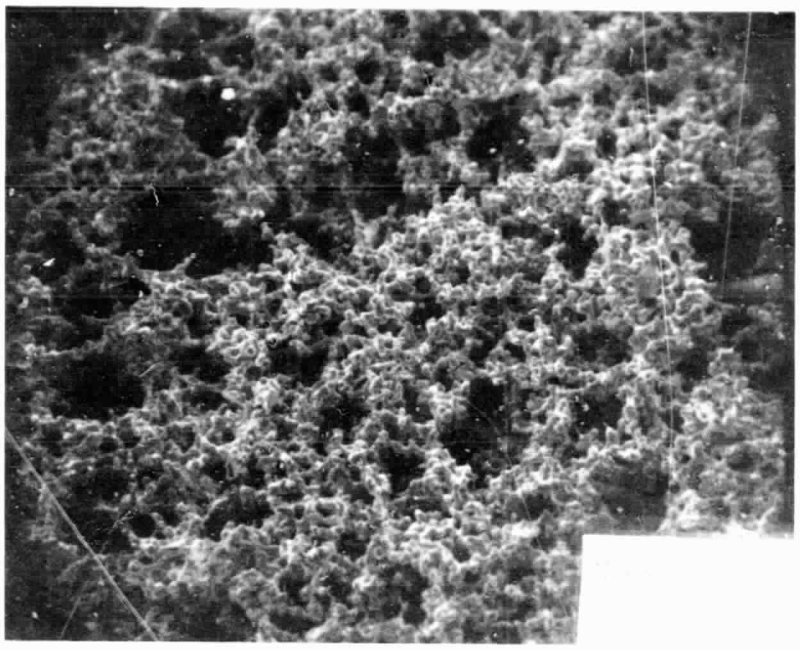

Figure 9—Smooth side of nickel plaque at 300X.

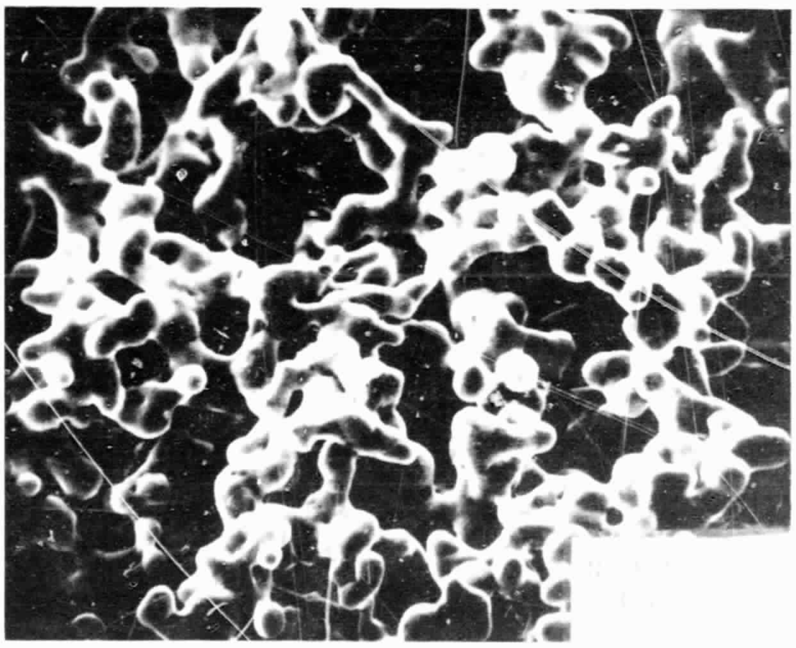

Figure 10—Smooth side of nickel plaque at 1550X.

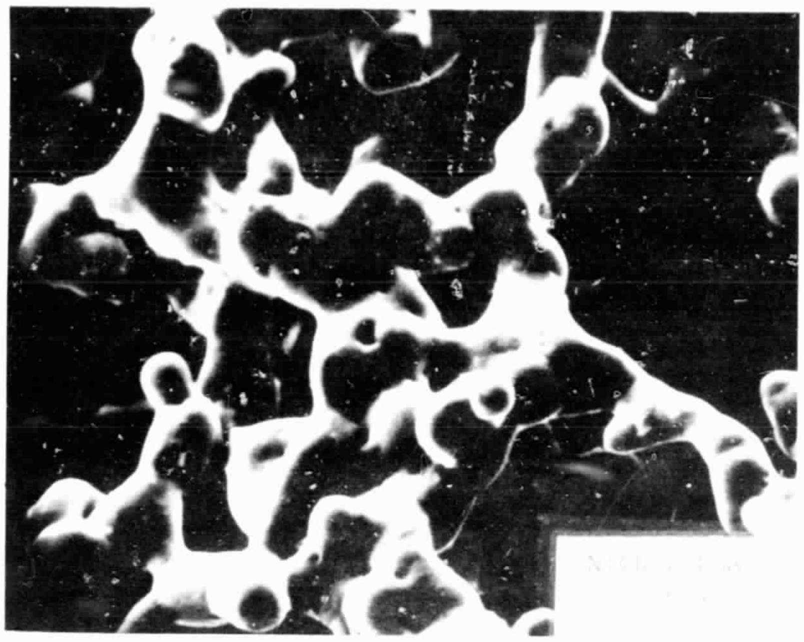

Figure 11—Smooth side of nickel plaque at 3200X.

Figure 12—Smooth side of nickel plaque at 7800X.

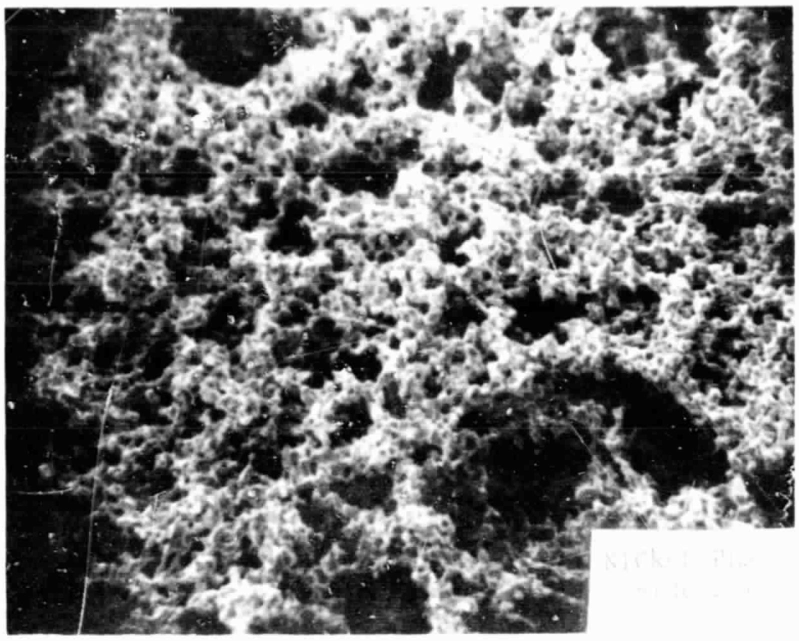

Figure 13—Rough side of nickel plaque at 300X.

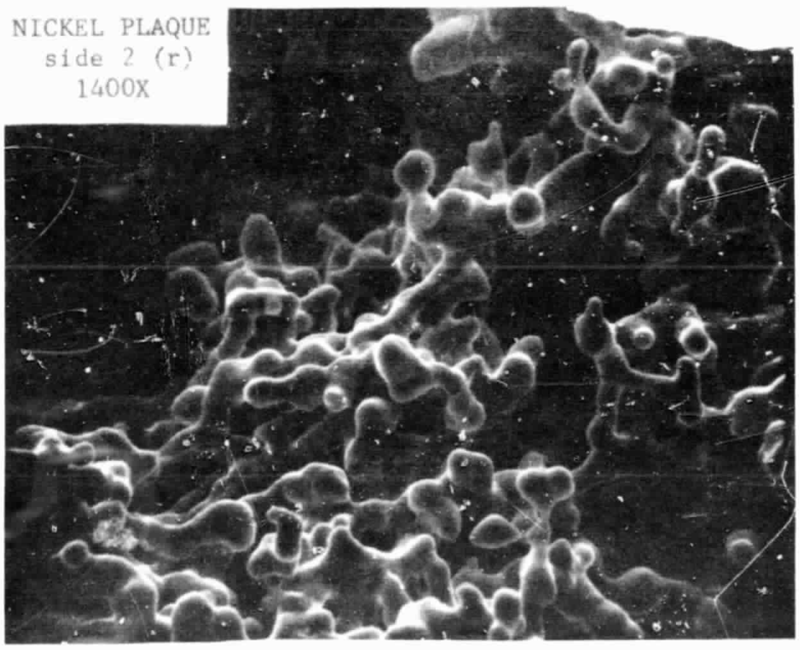

Figure 14—Rough side of nickel plaque at 1400X.

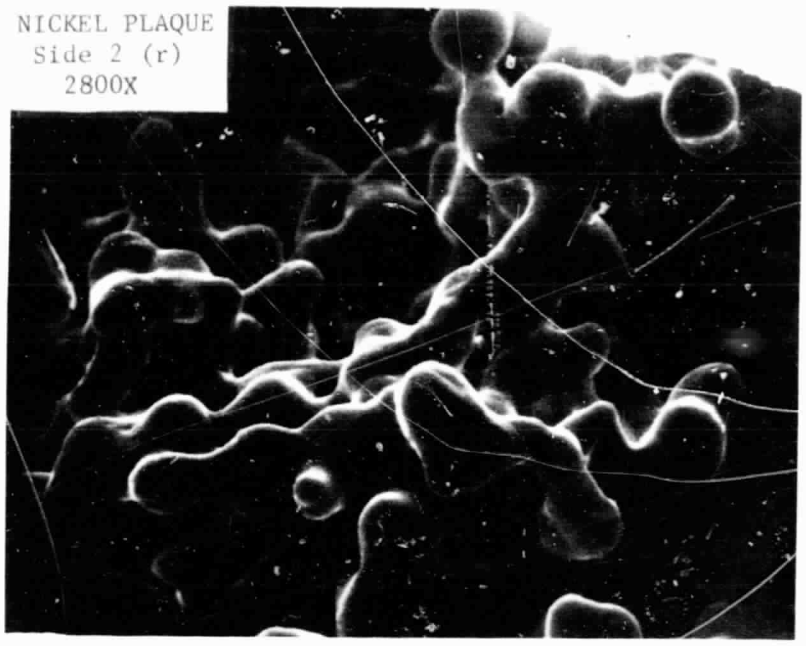

Figure 15—Rough side of nickel plaque at 2800X.

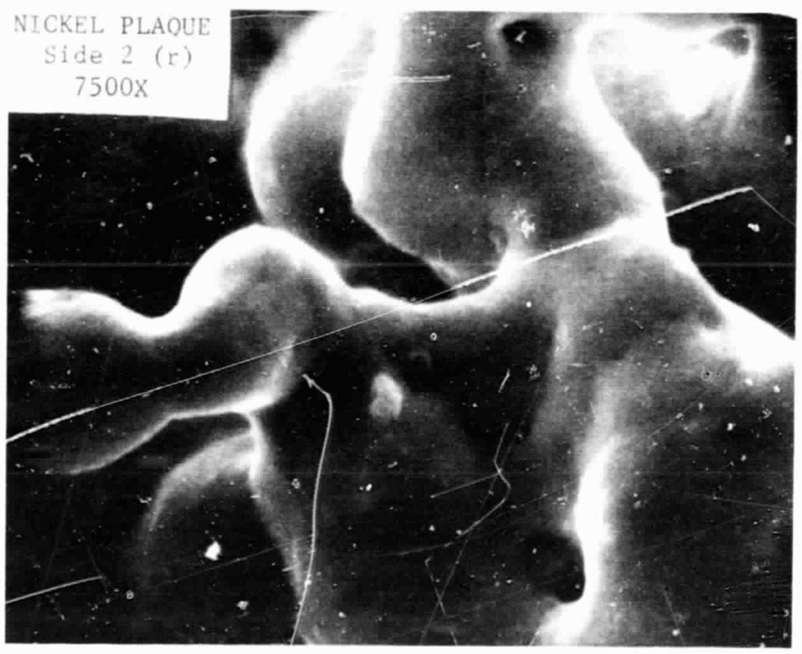

Figure 16—Rough side of nickel plaque at 7500X.